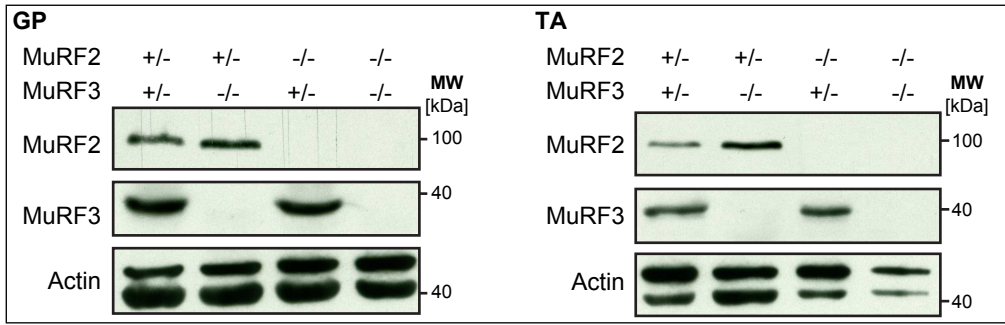
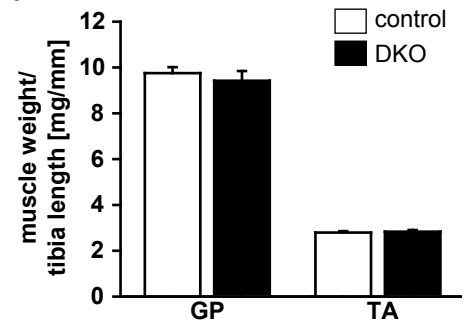
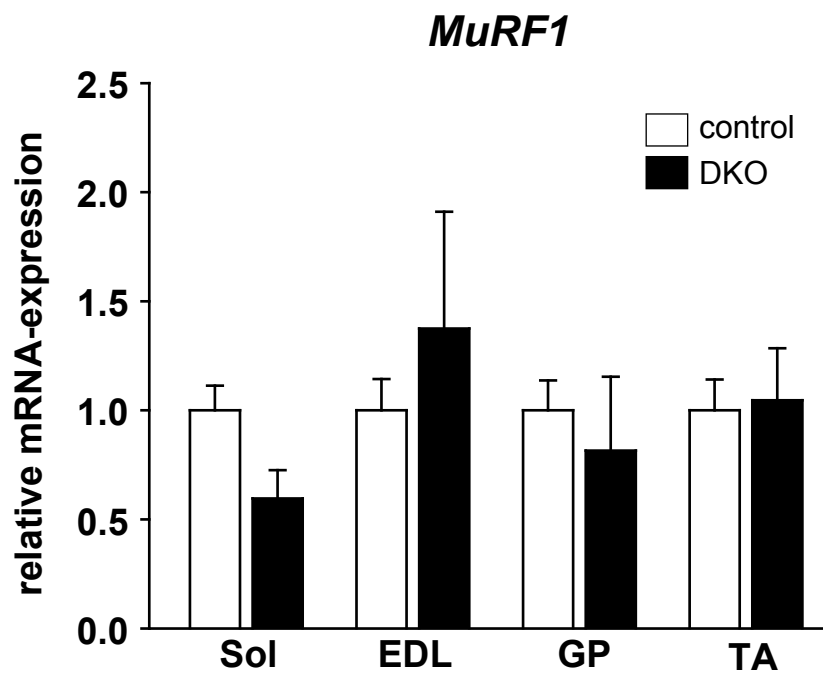
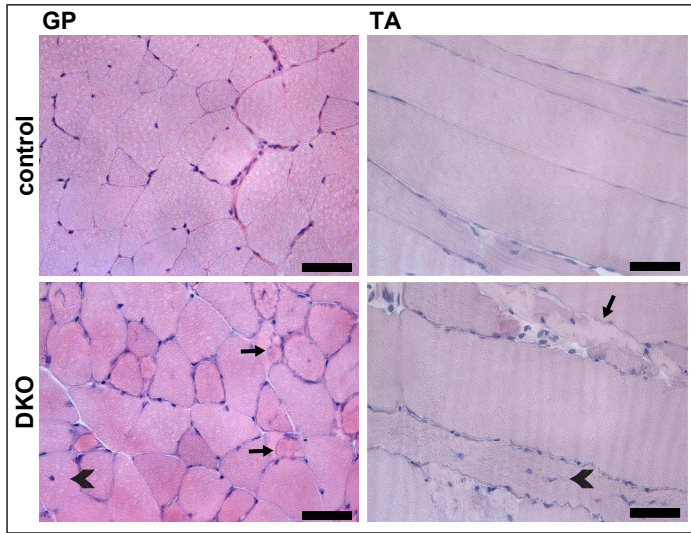
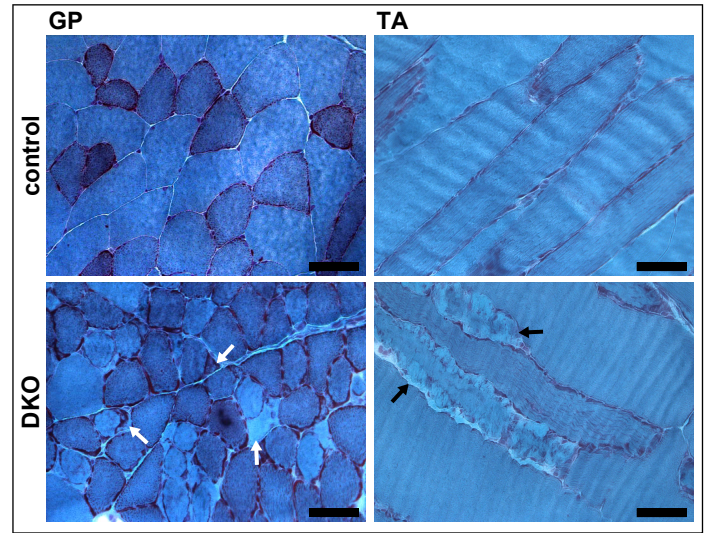
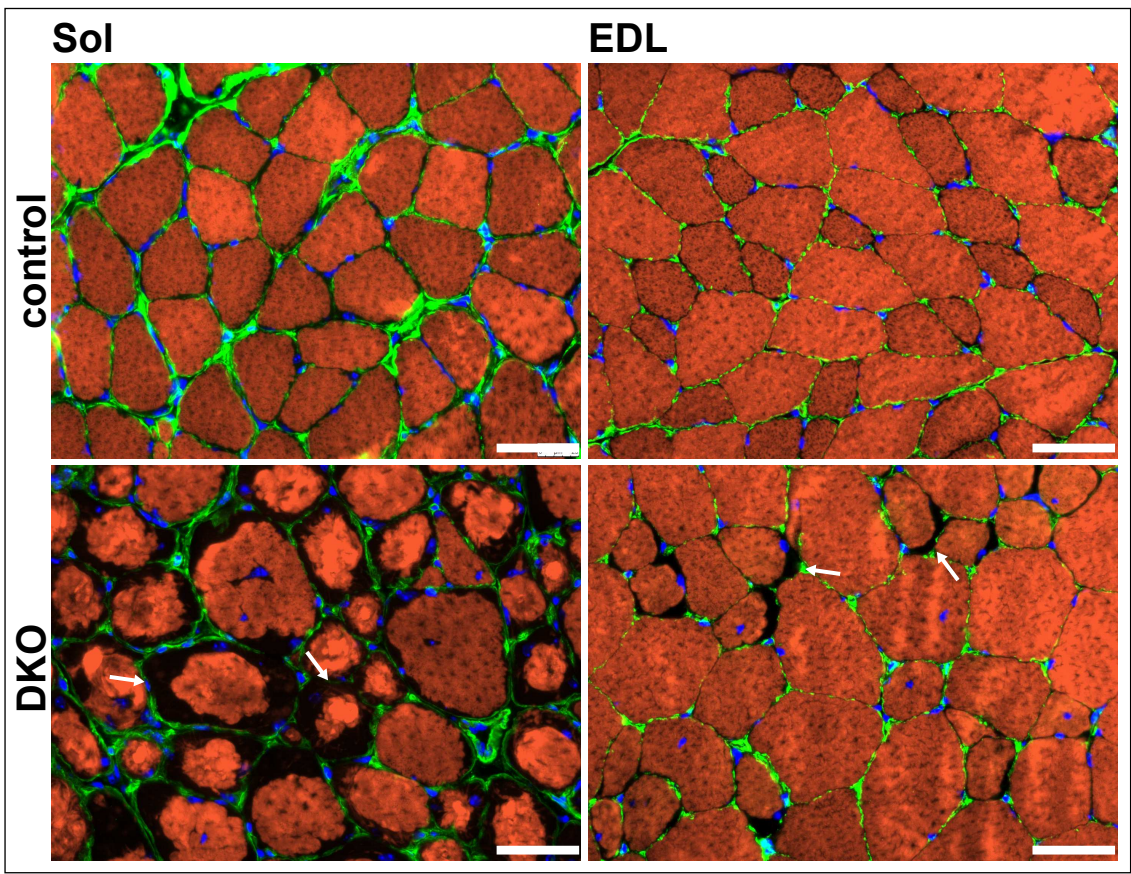


**a****b****Fig. S1**



**Fig. S2**

**a****b****Fig. S3**



**Fig. S4**

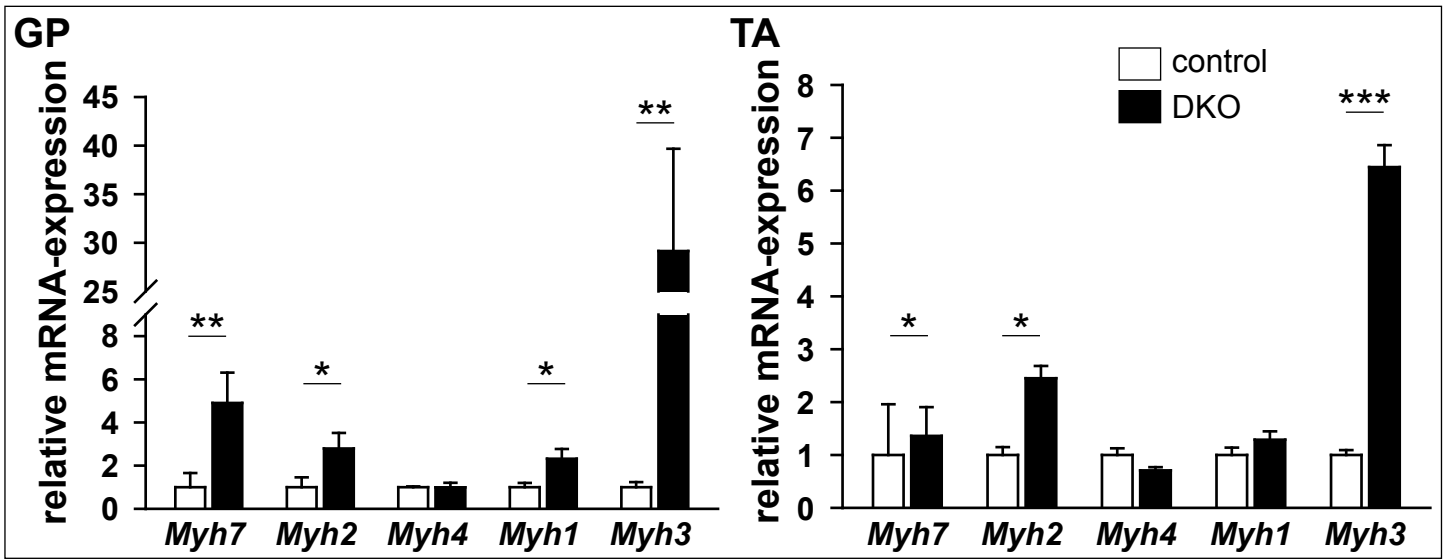


Fig. S5

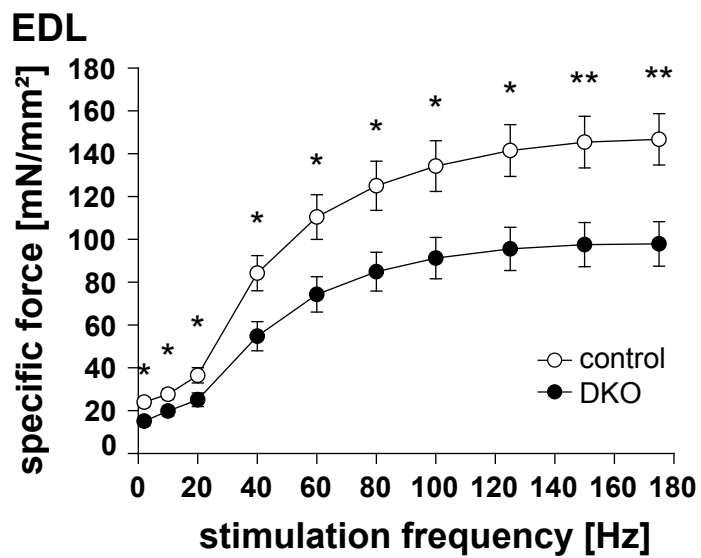
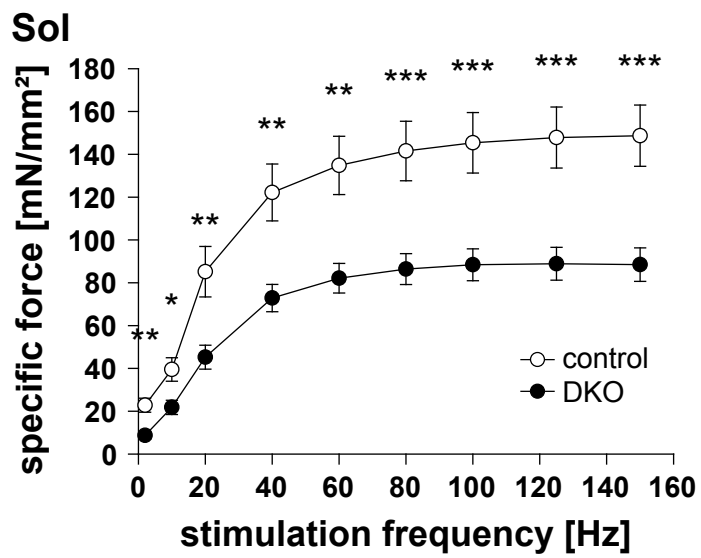
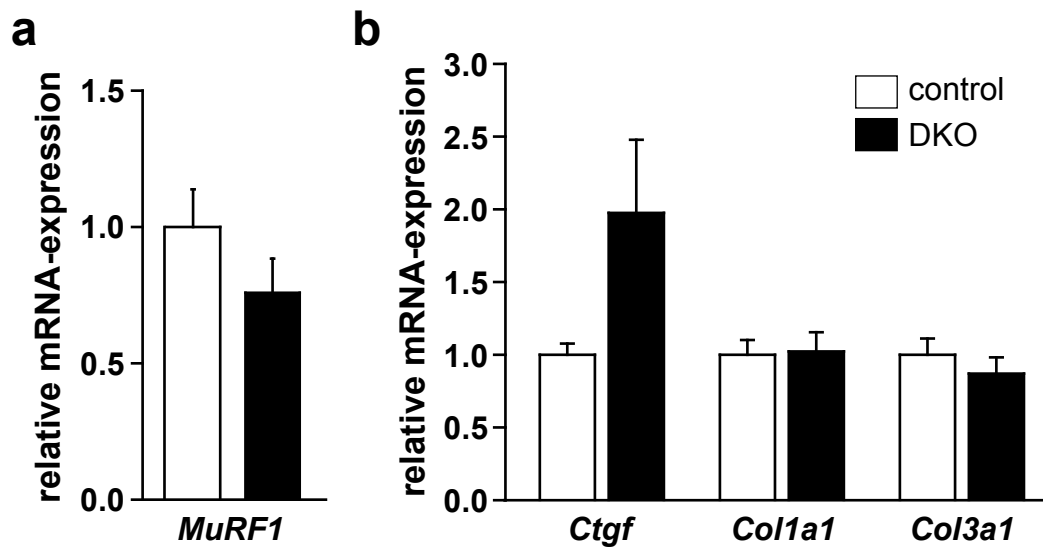


Fig. S6



**Fig. S7**

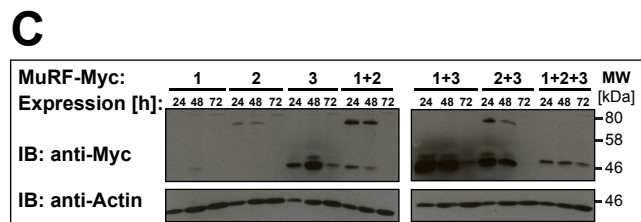
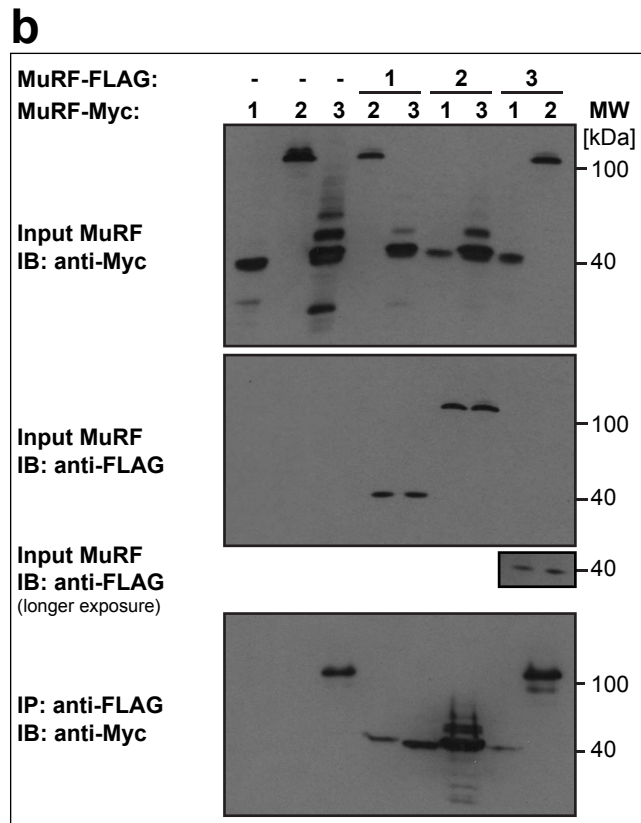
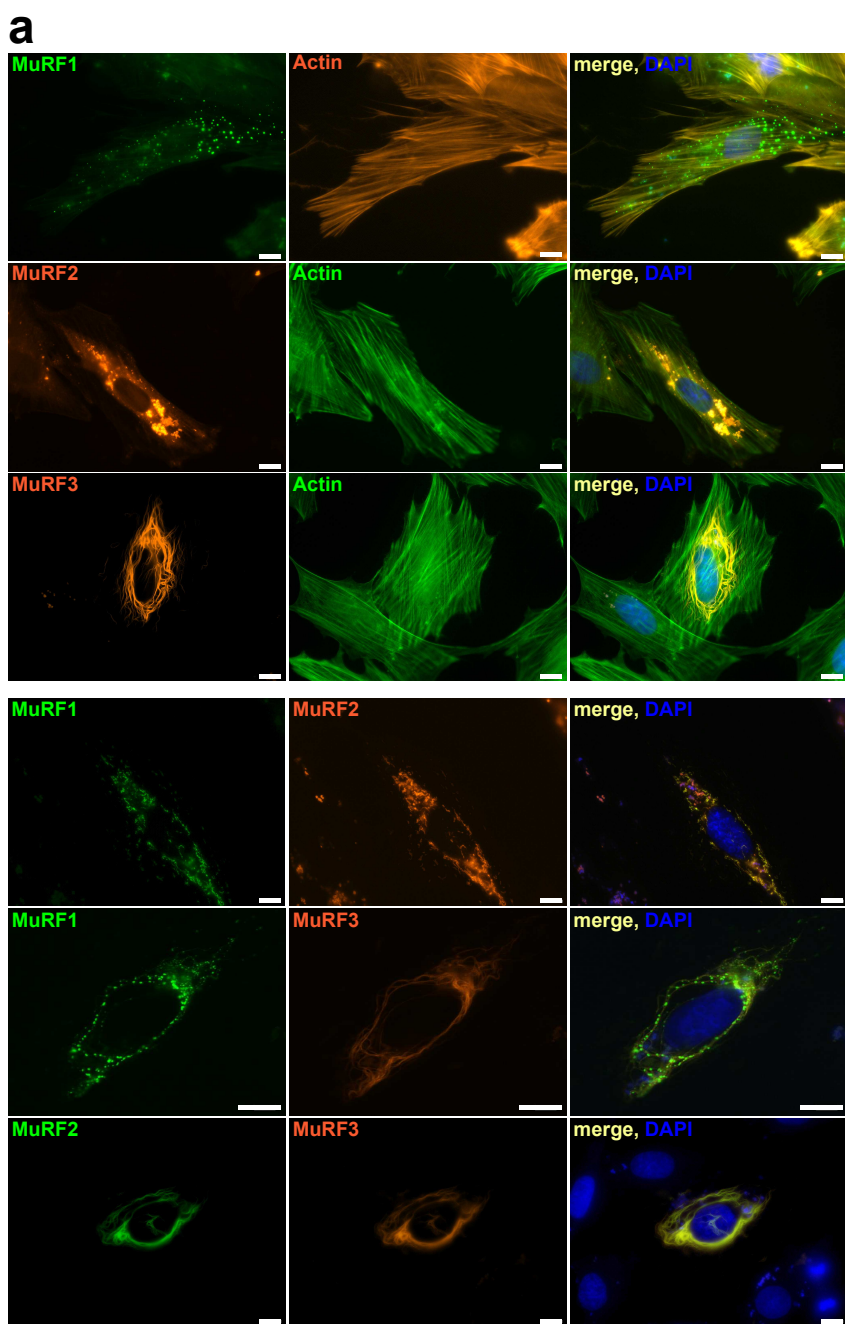
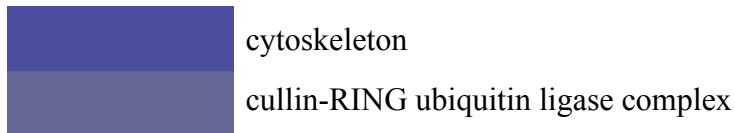


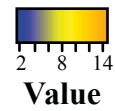
Fig. S8

## a GO-term analysis of proteins upregulated in DKO muscle

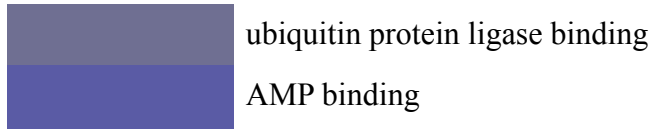
### $\alpha$ Cellular component



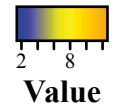
### Color Key



### $\beta$ Molecular function

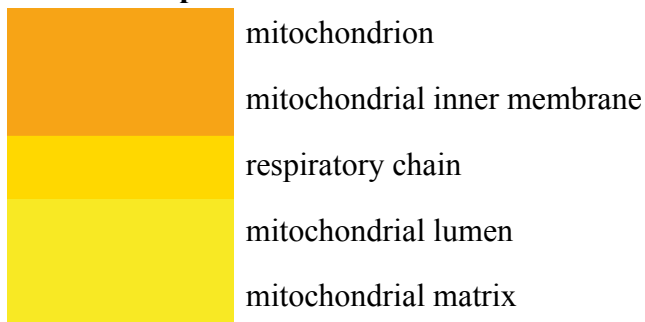


### Color Key

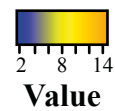


## b GO-term analysis of proteins downregulated in DKO muscle

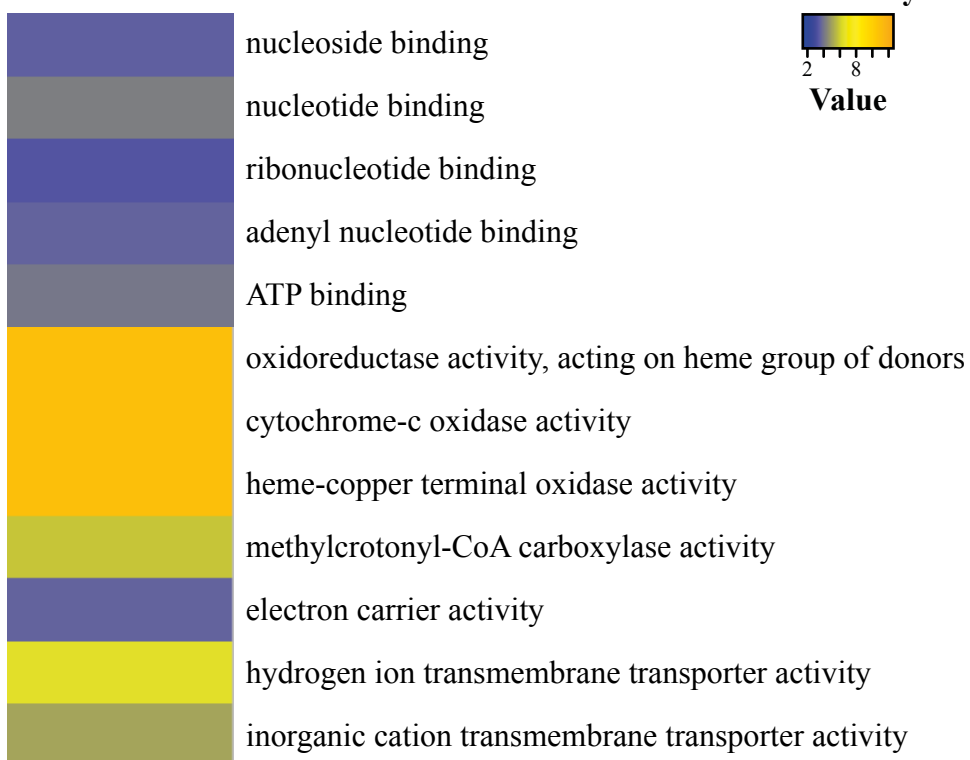
### $\alpha$ Cellular component



### Color Key



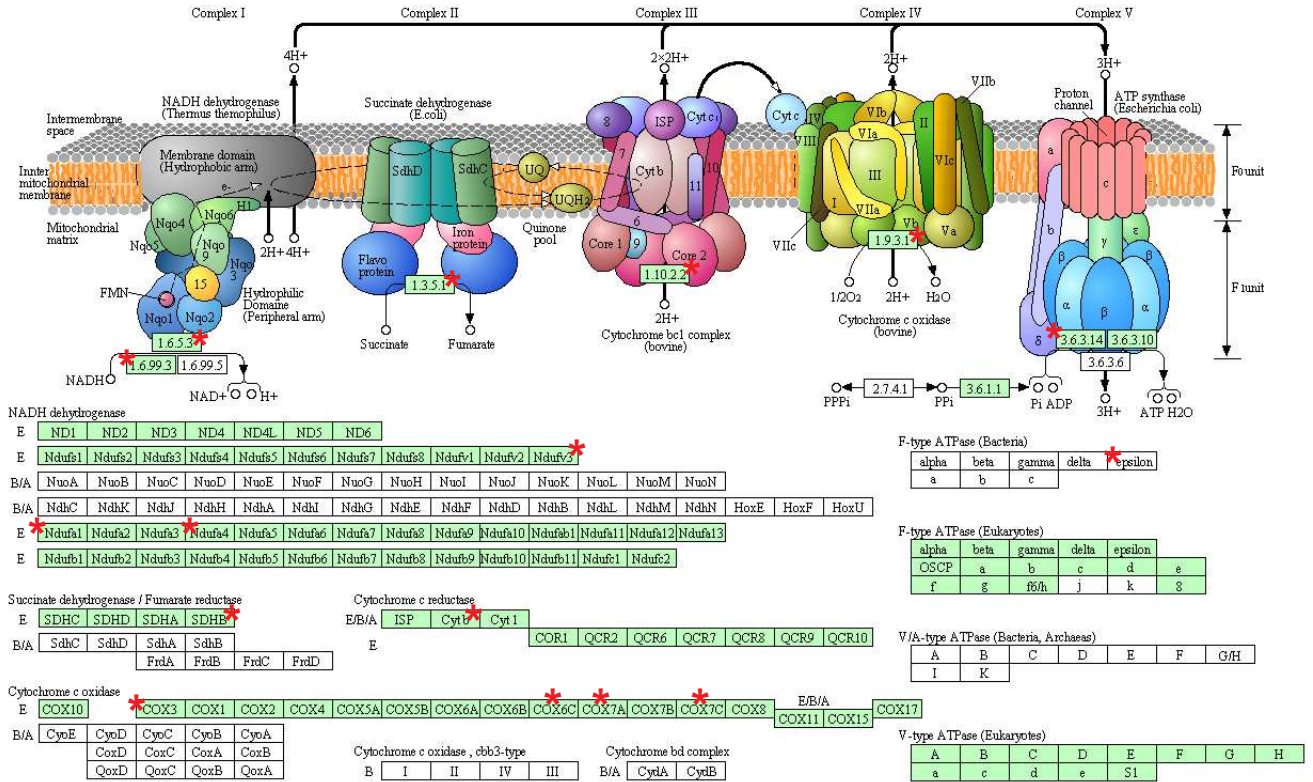
### $\beta$ Molecular function



### Color Key



OXIDATIVE PHOSPHORYLATION



00190 5/7/14  
(c) Kanehisa Laboratories

Fig. S10

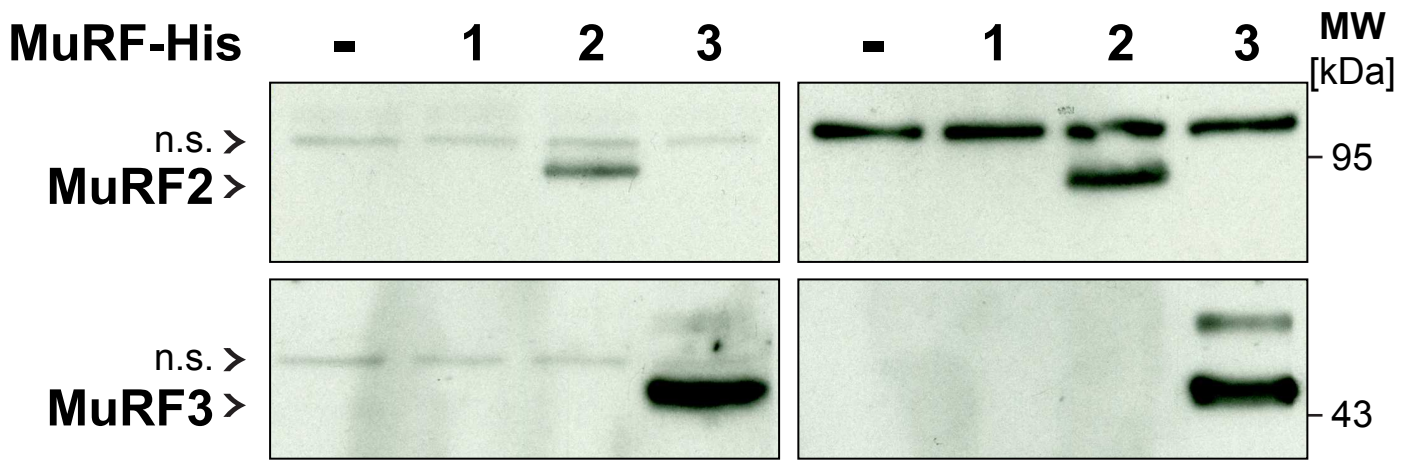


**Fig. S11**

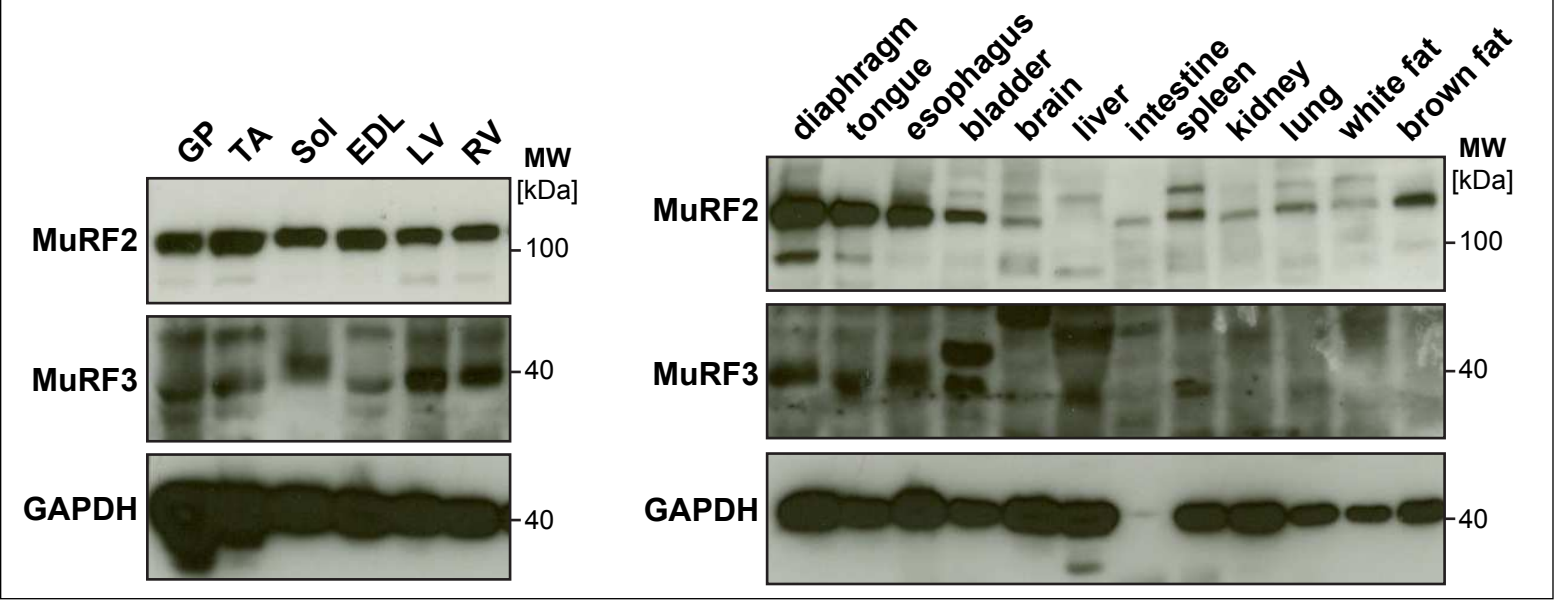


Fig. S12

### Supplemental materials and methods

**Generation of antibodies.** Peptide specific anti-MuRF2 and anti-MuRF3 antibodies were generated by immunizing rabbits with MuRF2 or MuRF3 specific peptides (BioGenes GmbH, Germany). Shortly, single MuRF2 or MuRF3 specific peptides (sequences are available upon request) were used for the intramuscular immunization of two rabbits each using BioGenes' adjuvant immunization. The adjuvant was mixed 3:1 with either antigen. Standard immunization was done over 35 days followed by blood sampling and harvesting of serum. Affinity purification of the serum was performed against the respective peptide. Purified antibodies were stored in Tris-Glycine buffer (pH 7.5) containing 250 mM NaCl and 0.02 % thimerosal. Specificity of both antibodies was confirmed by Western blot analyses using lysates from MuRF1, MuRF2 or MuRF3 overexpressing COS-7 cells (Figure S11) and lysates of *soleus*, *extensor digitorum longus* (Figure 1A), *tibialis anterior*, and *gastrocnemius/plantaris* (Figure S1A) from *MuRF2* and *MuRF3* germline deleted mice. More precisely, the anti-MuRF2 antibody detected overexpressed MuRF2 but not MuRF1 or MuRF3. Likewise, the anti-MuRF3 antibody detected overexpressed MuRF3 but not MuRF1 or MuRF2 (Figure S11). Accordingly, no specific immunoreactive band was found in muscular protein lysates from MuRF2 knockout mice with the anti-MuRF2 antibody, and from MuRF3 knockout mice with the anti-MuRF3 antibody (Figure 1A). With these antibodies we confirmed muscle specific expression of MuRF2 and MuRF3 by Western blot analysis (Figure S12).

**Muscle dissection.** *Soleus*, *extensor digitorum longus*, *tibialis anterior*, and *gastrocnemius/plantaris* were harvested from control and DKO mice, weighted and either snap frozen in liquid nitrogen for RNA and protein isolation or embedded in gum tragacanth

(Synopharm GmbH, Germany) for histological analyses. In addition, hearts were harvested and treated accordingly. Tibia length was measured and used for normalization of muscle weights.

**Protein purification.** The FastPrep-24™ instrument (MP Biomedicals, CA, USA) was used to homogenise muscle tissue in lysis buffer (50 mM Tris, pH 7.5, 150 mM NaCl, 10 % glycerol, 1 % Triton X-100, pH 7.5) supplemented with protease inhibitors (cOmplete; Roche Diagnostics GmbH, Germany) using Micro Packaging Vials with 2.8 mm Precellys ceramic beads (PEQLAB Biotechnology GmbH, Germany). Lysates were cleared by centrifugation at 16.000 g for 20 min at 4° C. Protein content in the supernatant was quantitated using Pierce® BCA reagent (Thermo Fischer Scientific Inc., MA, USA). Proteins were stored at -80°C.

For analysis of endogenous MAPKAPK2, MAPKAPK3 and p38 MAPK tissue from left ventricle and *soleus* were homogenised in 150 µl kinase lysis buffer (20 mM TRIS-acetat pH 7.0, 0.1 M EDTA, 1 mM EGTA, 1 mM Na<sub>3</sub>VO<sub>4</sub>, 10 mM β-glycerophosphate, 50 mM NaF, 5 mM sodium pyrophosphate, 1 % Triton X-100, 1 mM benzamidine, 2 µg/ml leupeptine, 0.1 % 2-Mercaptoethanol, 0.27 M saccharose, 0.2 mM PMSF) supplemented with aluminium oxide and protease inhibitors (cOmplete; Roche Diagnostics GmbH, Germany). Lysates were cleared by centrifugation at 15.000 g for 20 min at 4° C. Protein content in the supernatant was quantitated using Bradford assay. Proteins were stored at -80°C. This protocol was recently published [1].

**Mass spectrometry of muscle proteins.** The FastPrep-24™ instrument (MP Biomedicals, California, USA) was used to homogenise *soleus* muscle of control (n = 3) and DKO (n = 3)

mice in denaturation buffer (10 mM HEPES, 6 M urea, 2 M thiourea, 2 % SDS) using Micro Packaging Vials with 2.8 mm Precellys ceramic beads (PEQLAB Biotechnology GmbH, Germany). Lysates were cleared by centrifugation at 16.000 g for 20 min at 4° C. The supernatant was precipitated using ethanol precipitation. The protein pellet was resuspended in denaturing buffer. Disulfide bridges were reduced using 10 mM DTT followed by an alkylation step using 55mM chloroacetamide. Proteins were digested following a two step protocol, first digesting using endopeptidase LysC (Wako, 1 µg/50 µg protein), followed by a dilution step reducing the urea content to 2 M urea and finally digesting the sample using trypsin (Promega, 1 µg/50 µg protein). Peptides were purified as described in Rappsilber et al 2007 [2]. After elution from the stage-tip cartridges, the peptides were separated on a reverse phase chromatography system using nano-flow Proxeon nLC-II system, Thermo Scientific, in-house prepared reverse-phase-column 15 cm, 75 µm, C18, 3 µm bead size, Dr. Maisch HPLC GmbH). The separated peptides were ionized on a proxeon ion source. MS and MS/MS spectra were recorded using a Q-Exactive mass spectrometer (Thermo Scientific) using higher energy collision dissociation method (HCD) of the top 10 most prominent ions. The recorded spectra were analysed using the MaxQuant software package (version 1.2.2.5) using the IPI human database, with carbamidomethylation of cysteins as a fixed and oxidation of methionines as a variable modification. For peptides and proteins a FDR of 1 % was applied.

**Bioinformatic analysis of mass-spectrometry data.** Data obtained from the MaxQuant analysis were used to identify significantly regulated proteins in DKO compared to control *soleus*. Proteins with a log<sub>2</sub>-fold change in abundance were considered significant if they were above or below the arbitrarily cut-off of 0.7 or -0.7 for up- and down-regulated proteins,

respectively. Three replicates were used to calculate significances using the non-parametric Wilcoxon-Mann-Whitney-Test. Proteins with a  $-\log_{10}(\text{p-value}) > 1$  were considered significantly regulated. These significantly regulated proteins were used for the Gene Ontology (GO) analysis using the DAVID online tool [3]. GO-terms with a score of more than 3.5 were clustered using Euclidian hierarchical clustering, combining all three branches of the GO annotations (biological processes, cellular component and molecular functions).

#### **Affinity chromatography for quantitation of MAPKAPK2 and MAPKAPK3 in muscle.**

Enrichment of MAPKAPK2 and MAPKAPK3 was performed as previously shown [1].

Shortly, the GST-p38 $\alpha$ -fusion protein and 25  $\mu\text{l}$  of prewashed Glutathion-Sepharose 4B (GE Healthcare) were used to co-purify MAPKAPK2 and MAPKAPK3 from muscle lysates.

Immunoprecipitation was performed in IP-buffer (25 mM TRIS-HCl, pH 7.4, 137 mM NaCl, 2.7 mM KCl, 50 mM NaF, 1 % Triton X-100) for 12 hours at 4°C. Afterwards sepharose was washed 3 times with IP-buffer. To elute bound proteins sepharose was heated to 95°C for 5 min in 20  $\mu\text{l}$  of SDS sample buffer (200 mM TRIS-HCl, pH 6.8, 8 % SDS, 40 % glycerol, 10 % 2-Mercaptoethanol, 0.08 % Bromophenol blue).

**Western blot analysis.** Western blot analysis was performed on protein samples from skeletal muscles, hearts and cells, as previously described [4]. Shortly, proteins were resolved by SDS-PAGE and transferred onto nitrocellulose membranes (GE healthcare, Germany). Membranes were blocked with either 5 % skim milk powder or 5 % bovine serum albumine (BSA) dissolved in TBS-T for 1 hour. Following primary antibodies were used for immunoblotting: anti-MuRF2 (polyclonal, rabbit, 1:300, own production), anti-MuRF3 (polyclonal, rabbit, 1:300, own production), anti-actin (monoclonal, mouse, 1:2000, Sigma-

Aldrich Chemie GmbH, Germany), anti- $\beta$ /slow MyHC (NOQ7, detecting skeletal slow myosin, monoclonal, mouse, 1:1000; Sigma-Aldrich Chemie GmbH, Germany), anti-pan MyHCII (My32, detecting skeletal fast myosin, monoclonal, mouse, 1:1000; Sigma-Aldrich Chemie GmbH, Germany), anti-MAPKAPK2 (polyclonal, rabbit, 1:1000, Cell Signaling Technology Inc., Danvers, USA), anti-p38 MAPK (polyclonal, rabbit, 1:1000, Cell Signaling Technology Inc., Danvers, USA), antibody. Loading was controlled with anti-GAPDH (clone 6C5, monoclonal, mouse, 1:50.000; Millipore GmbH, Germany), anti-GAPDH (monoclonal, mouse, 1:1000, Biotrend Chemicals, LLC, Destin, FL, USA; for MAPKAPK analysis) and anti-tubulin (clone TU-02, monoclonal, mouse, 1:1000; Santa Cruz Biotechnology, Inc., Santa Cruz, CA, USA) antibody. HRP-linked IgG horse anti-mouse, goat anti-rabbit (both 1:2000, Cell Signaling Technology Inc., Danvers, USA) or rabbit anti-goat (1:5000, Abcam, UK) were used as secondary antibody. Proteins were visualized with a chemiluminescence system (SuperSignal® West Pico Chemiluminescent substrate, Thermo Fischer Scientific Inc., MA, USA). For the detection of MAPKAPK3, we performed p38-GST-pulldown assays with cell lysates followed by Western blot analysis using an anti-MAPKAPK3 antiserum as described previously [5].

**Gene expression analyses by real-time RT-PCR.** Total RNA was isolated from heart and skeletal muscles using TRIzol® Reagent (Invitrogen™, Life Technologies Corporation, CA, USA) and the FastPrep-24™ instrument in accordance with manufacturer's instructions. 1  $\mu$ g of RNA was reverse transcribed (Superscript® II Reverse Transcriptase, Invitrogen™, Life Technologies Corporation, CA, USA) in accordance with manufacturer's instructions. Real-time PCR was performed using SYBR® Green (Roche Diagnostics GmbH, Germany) with primer sets (Table S1) and PCR conditions that have been previously reported [6].

*Hypoxanthine-guanine phosphoribosyltransferase (Hprt)* content was used as reference gene, and expression of specific genes was related to stably expressed *Hprt*.

**Histological and immunohistochemical analyses.** *Soleus*, *extensor digitorum longus*, *gastrocnemius/plantaris*, and *tibialis anterior* were harvested from control and DKO mice and either flash frozen in gum tragacanth (Sigma-Aldrich Chemie GmbH, Germany) or fixed in 4% paraformaldehyde and processed for routine paraffin histology as described previously [7]. Frozen sections were cut on a cryotome (Leica CM 3050 S, Leica Microsystems GmbH, Germany) and stained with hematoxylin and eosin, metachromatic ATPase dye or modified Gomori's trichrome as previously described [7]; Gomori One-Step Trichrome with Light Green was purchased from Sigma-Aldrich Chemie GmbH, Germany. Frozen histological sections were immunostained with anti- $\beta$ /slow MyHC (NOQ7, detecting skeletal slow myosin, monoclonal, mouse, 1:100), anti-pan MyHCII (My32, detecting skeletal fast myosin, monoclonal, mouse, 1:100) and anti-Laminin (polyclonal, rabbit, 1:200, all Sigma-Aldrich Chemie GmbH, Germany) primary antibody over night at 4°C. Goat anti-mouse and goat anti-rabbit IgG (Alexa Fluor 488 nm or 555 nm, 1:500, Invitrogen™ Life Technologies Corporation, CA, USA) were used as secondary antibody. Filamentous actin was stained with phalloidin-TRITC (2.5  $\mu$ g/100  $\mu$ l, Sigma-Aldrich Chemie GmbH, Germany). Images were acquired with a Leica CTR 6500 HS microscope, and Leica digital camera DFC 425 for histological analyses and Leica digital camera DFC 360 FX for fluorescence pictures (Leica Microsystems GmbH, Germany). Analyses of images were performed with ImageJ software 1.42c (<http://rsb.info.nih.gov/ij/>). Myocyte cross-sectional area (MCSA) was measured from *extensor digitorum longus* from at least 100 myofibres per genotype and histological section. Centralized nuclei were quantitated in 60-270 myofibres per genotype and histological

section from both *soleus* and *extensor digitorum longus*. Fibre type composition was determined in 330-970 myofibres per genotype and histological section from *soleus* and *extensor digitorum longus*.

**Electron microscopy.** 4-6 month old male and female control and DKO mice were anesthetized and systemically perfused with 4 % formaldehyde, 1.25 % glutaraldehyde in 0.08 M phosphate buffer. *Soleus* and *extensor digitorum longus* as well as the interventricular septum of the heart were dissected and postfixed with 2.5 % glutaraldehyde in 0.1 M phosphate buffer for 3 days at 4°C. Following washing and transfer into 0.1 M cacodylate buffer, tissue was stained with 1 % osmium tetroxide for 2 hours, dehydrated in a graded ethanol series and propylene oxide and embedded in Poly/Bed<sup>®</sup> 812 (Polysciences, Inc., Germany). Ultrathin sections (60 nm) were contrasted with uranyl acetate and lead citrate and examined with a FEI Morgagni electron microscope. Digital images were taken with a Morada CCD camera and the iTEM software (Olympus Soft Imaging Solutions GmbH, Germany).

**Measurement of muscle force.** Muscle force measurements were performed as previously described [6]. To compare muscle function of control and DKO mice male and female littermates were analysed. The *soleus* and *extensor digitorum longus* were isolated and immediately attached to a force transducer and positioned between two steel electrodes (800A *in vitro* test apparatus, 701C High-Power, Bi-Phase Stimulator, 300C Dual-Mode Muscle Lever System, Aurora Scientific). The muscles were continuously perfused with oxygenated (95 % O<sub>2</sub> and 5 % CO<sub>2</sub>) physiological salt solution (modified Krebs-Henseleit buffer: 112 mM NaCl, 4.5 mM KCl, 1.2 mM MgSO<sub>4</sub>, 2.5 mM CaCl<sub>2</sub>, 1.2 mM NaH<sub>2</sub>PO<sub>4</sub>, 26 mM

NaHCO<sub>3</sub>, 11 mM glucose) at 25°C and pH 7.4 [8]. Muscles were allowed to equilibrate for 15 min in the modified Krebs-Henseleit buffer. Then, the optimal length at which the muscle generates a maximum twitch force was determined for each muscle investigated ( $L_0$ ). This specific individual muscle length was used for all subsequent measures. Second, muscles were allowed to recover for 10 min. Third, *soleus* was stimulated with various increasing frequencies (2, 10, 20, 40, 60, 80, 100, 125, and 150 Hz) and force development was measured. The *extensor digitorum longus* underwent the same protocol plus an additional 175 Hz stimulus. Resting periods of 1.5 min were applied between individual stimulation steps. Force development was normalised to calculated muscle cross-sectional area (CSA) as described by others [9]. Briefly, CSA was calculated by dividing muscle mass in mg by optimal length  $L_0$  in mm, the density of skeletal muscle (1.06 g/cm<sup>3</sup>) and the ratio of myofibre length to muscle length which is 0.45 and 0.71 for *extensor digitorum longus* and *soleus*, respectively [9]. Data are depicted as force-frequency curves.

**Isolation of adult mouse ventricular cardiomyocytes.** Ventricular cardiomyocytes were isolated from hearts of 15-week old male DKO mice and control littermates as described previously [10]. All experiments followed the guidelines of the German State Department for Animal Protection and Welfare as well as the German Society for Experimental Animal Science and were in accordance with Federal German Animal Protection Law (GV-SOLAS, TSchG). The experimental protocol was approved by the University Committee on Use and Care of Animals at the Hannover Medical School and the Lower Saxony State Board on the Care and Use of Animals (LAVES, Oldenburg, Germany; #33.9-42502-04-11/0358). Mice were anesthetized with isoflurane (Baxter, Germany) using a vaporizer (E-Z-systems Corp., PA, USA) and anticoagulated with 500 U heparin sodium *i.p.* After a bilateral thoracotomy

the aorta thoracalis was cannulated within 30 seconds and the heart perfused on a pressure-constant Langendorff apparatus (50 mmHg, flow: 3 ml/min) with calcium-free Krebs-Henseleit buffer (118 mM NaCl, 4.7 mM KCl, 21 mM NaHCO<sub>3</sub>, 1.2 mM MgSO<sub>4</sub>, 11 mM glucose, 1.2 mM KH<sub>2</sub>PO<sub>4</sub> and 10 mM taurine 5, 2,3-butanedione monoxime; pH 7.4) equilibrated with carbogen (5 % CO<sub>2</sub>, 95 % O<sub>2</sub>) at 37°C. After 4 min of perfusion enzymatic digestion with collagenase type II (140 U/ml, Lot M8B10274 Worthington Biochemical Corp., NJ, USA) and hyaluronidase type I-S (52 U/ml, Lot 029K77001, Sigma-Aldrich Chemie GmbH, Germany) diluted in Ca<sup>2+</sup>-free Krebs-Henseleit buffer was initiated. After 8 min of digestion, extracellular Ca<sup>2+</sup> was increased in two steps to a final concentration of 0.7 mM and the perfusion continued for additional 5 min. The left ventricle was minced and resuspended in 5 ml of enzyme containing Krebs-Henseleit buffer. Cardiomyocyte dissociation was achieved by triturating the tissue (2 min, 37 °C) using sterile silanized glass pipettes. The resulting cell suspension was washed twice using centrifugation (30 g, 1 min) and resuspension in Ca<sup>2+</sup>-containing Krebs-Henseleit buffer supplemented with 2 % and 6 % bovine serum albumin. Finally, cardiomyocytes were resuspended in DMEM containing 0.9 mM Ca<sup>2+</sup> (mixture of E 15810 and E 15078: PAA-Laboratories, Austria), supplemented with 1 % antibiotics (Penicillin/Streptomycin, Biochrom AG, Germany, 10,000 µg/ml). Cardiomyocytes were cultured in M199 (E15-838, PAA-Laboratories), pH 7.4, supplemented with 10 mM glutathione, 0.2 mg/ml BSA, 1 % antibiotic solution (Pen/Strep, Biochrom AG, Germany, 10,000 µg/ml) and plated onto laminin coated coverslips (40 µg/ml, Invitrogen™, USA). Cultures were incubated at 37°C in 5 % CO<sub>2</sub>. Only quiescent, rod-shaped myocytes were subjected to measurements within 10 hours. Cell size was determined by measuring length and width of cardiomyocytes from pictures obtained directly after the isolation procedure.

**Measurements of single cell contraction and calcium transients of adult cardiomyocytes.**

Cell contractions and calcium transients were measured as described previously [10]. Briefly, contractile properties of cardiomyocytes in culture were measured with the IonOptix system (IonOptix Corporation, USA) equipped with a camera connected to an inverted microscope (Olympus IX71, Olympus Corporation, Japan) and sarcomere length detection software (IonWizard®, IonOptix Corporation, USA). A coverslip with plated cardiomyocytes was placed in a prefabricated chamber slowly perfused with buffer solution (117 mM NaCl, 5.7 mM KCl, 1.2 mM NaH<sub>2</sub>PO<sub>4</sub>, 0.66 mM MgSO<sub>4</sub>, 10 mM glucose, 5 mM sodiumpyruvat, 10 mM creatin, 20 mM HEPES, 1.25 mM CaCl<sub>2</sub>, 0.03 mM ascorbic acid, pH 7.4) at 37 °C. Temperature stability in the closed chamber was continuously monitored and automatically maintained by a temperature controller (CellMicroControls, USA). Myocytes were paced with 5 Hz at supramaximal voltage and 4 ms impulse duration (MyoPacer, IonOptix Corporation, USA). Sarcomeric contractions were recorded at 5 Hz for 30 s. The parameters analysed included peak sarcomere shortening as amplitude, and contraction and relaxation velocity after averaging 20 transients per cardiomyocyte.

Ca<sup>2+</sup>-transients of cardiomyocytes were recorded simultaneously with sarcomere shortening using a dual excitation fluorescence photomultiplier system (IonOptix Corporation, USA) with 1.5 µM fura-2 AM (Invitrogen™ Corp., Molecular probes®, OR, USA) and 15 min loading time at 37°C. Afterwards, cells were washed twice with M199. The fluorescence emitted at 510 nm after alternating excitation wavelength between 340 nm and 380 nm was measured. Average background fluorescence obtained from 10 untreated cells was subtracted and the ratio (340nm/380nm) calculated as described [11]. From the ratio transients, which

indicate the free intracellular  $\text{Ca}^{2+}$ -transients we analysed ratio amplitude, maximum velocity of  $\text{Ca}^{2+}$ -transient increase and maximum velocity of  $\text{Ca}^{2+}$ -transient decrease. For each condition 20 transients were averaged using the IonWizard<sup>®</sup> software (IonOptix Corporation, USA).

**Body composition.** Body composition was measured in 5 month old male DKO ( $n = 4$ ) mice and their control littermates ( $n = 8$ ) using the LF90 II time domain NMR analyser (6.5 MHz, Bruker Optics, USA) [12]. Awake mice were placed into the restraint tube which was adjusted to minimize movements of the animal without impairing respiration. The tube together with the animal was placed into the LF90 II instrument, and fat mass, fat-free (equal to muscle) mass and fluid were measured in triplicate.

**Langendorff.** The Langendorff heart experiments were performed as recently described [13]. In short, 2 month old male DKO ( $n = 6$ ) mice and their control littermates ( $n = 4$ ) were anaesthetized using 100 mg/kg ketamine and 10 mg/kg xylazin 2 %. 250 I.U. Heparin injected *i.p.* was used for anticoagulation. Hearts were excised immediately and transferred to a dissection dish containing ice-cold modified Krebs-Henseleit buffer (118.0 mM NaCl, 4.7 mM KCl, 2.0 mM  $\text{CaCl}_2$ , 2.1 mM  $\text{MgSO}_4$ , 24.7 mM  $\text{NaHCO}_3$ , 1.2 mM  $\text{KH}_2\text{PO}_4$ , 0.06 mM EDTA, and 10.0 mM glucose, pH 7.4). The aorta was retained to a primed 21 gauge stainless steel cannula still remaining in cold buffer. Hearts were mounted on the Langendorff perfusion rig and retrogradely perfused with modified Krebs-Henseleit buffer equilibrated with carbogen (5 %  $\text{CO}_2$ , 95 %  $\text{O}_2$ ) under constant perfusion pressure (60 mmHg). Temperature of the perfusate was adjusted to 37°C. Hearts were electrically stimulated with a coaxial electrode at 8.3 Hz (500 bpm). Correct position of the electrode at the sinus node was

assured by ECG recordings using two surface electrodes and a neutral zero electrode. To measure left ventricular pressure (LVP) a self-made balloon was passed through the mitral valve and inserted into the left ventricle. This balloon was connected to a calibrated pressure transducer (APT300, Hugo Sachs electronics, Germany) via a fluid filled tube. Other parameters were calculated based on the LVP such as maximum rate of pressure increase and pressure decrease ( $+dLVP/dt_{\max}$ ,  $-dLVP/dt_{\max}$ ). All data were acquired using the Isoheart software (Hugo Sachs Electronics, Germany). Hearts were allowed to recover for 20 min before measurements were performed. Only hearts with a developing pressure above 40 mmHg were used for analysis. After baseline measurements isoproterenol (ISO) was added via a syringe pump at a concentration of 50 nM.

**Table S1. Primer pairs for real time RT-PCR are shown.**

<b>Gene</b>	<b>Primer sequence</b>
<b>Mm_Coll1a1_forward</b>	5`-TGT AAA CAC CCC AGC GAA GAA-3`
<b>Mm_Coll1a1_reverse</b>	5`-CTG AGT TGC CAT TTC CTT GGA-3`
<b>Mm_Col3a1_forward</b>	5`-CTC ACC CTT CTT CAT CCC ACT CTT A-3`
<b>Mm_Col3a1_reverse</b>	5`-ACA TGG TTC TGG CTT CCA GAC AT-3`
<b>Mm_Ctgf_forward</b>	5`-TTC CCG AGA AGG GTC AAG CT-3`
<b>Mm_Ctgf_reverse</b>	5`-TTG GGT CTG GGC CAA ATG T-3`
<b>Mm_Hprt_forward</b>	5`-GCT TTC CCT GGT TAA GC AGT ACA-3`
<b>Mm_Hprt_reverse</b>	5`-ACA CTT CGA GAG GTC CTT TTC AC-3`
<b>Mm_Nppa_forward</b>	5`-GGG GGT AGG ATT GAC AGG AT-3`
<b>Mm_Nppa_reverse</b>	5`-ACA CAC CAC AAG GGC TTA GG-3`
<b>Mm_Nppb_forward</b>	5`-GCA CAA GAT AGA CCG GAT CG-3`
<b>Mm_Nppb_reverse</b>	5`-CTT CAA AGG TGG TCC CAG AG-3`
<b>Mm_MuRF1_forward</b>	5`-CCT GCA GAG TGA CCA AGG A-3`
<b>Mm_MuRF1_reverse</b>	5`-GGC GTA GAG GGT GTC AAA CT-3`
<b>Mm_Mapkapk2_forward</b>	5`-CAG CAA AAA TTC GCC CTA AA-3`
<b>Mm_Mapkapk2_reverse</b>	5`-AGT GCA GCT CCA CCT CTC TG-3`
<b>Mm_Mapkapk3_forward</b>	5`-CTG AAT GGT TAG ATG TCT CTG AGG-3`
<b>Mm_Mapkapk3_reverse</b>	5`-GCC TCT CTG TGG GAT CTG TC-3`
<b>Mm_Myh1_forward</b>	5`-AAT CAA AGG TCA AGG CCT ACA A-3`
<b>Mm_Myh1_reverse</b>	5`-GAA TTT GGC CAG GTT GAC AT-3`
<b>Mm_Myh2_forward</b>	5`-AAC TCC AGG CAA AAG TGA AAT C-3`
<b>Mm_Myh2_reverse</b>	5`-TGG ATA GAT TTG TGT TGG ATT GTT-3`
<b>Mm_Myh3_forward</b>	5`-AGAGGGTTTCTCATGCGTGT-3`
<b>Mm_Myh3_reverse</b>	5`-TGTTGTACTGGATGCAGAAGAT -3`
<b>Mm_Myh4_forward</b>	5`-TGG CCG AGC AAG AGC TAC-3`
<b>Mm_Myh4_reverse</b>	5`-TTG ATG AGG CTG GTG TTC TG-3`
<b>Mm_Myh6_forward</b>	5`-GCC AAG ACT GTC CGG AAT GA-3`
<b>Mm_Myh6_reverse</b>	5`-TGG AAG ATC ACC CGG GAC TT-3`
<b>Mm_Myh7_forward</b>	5`-CAA AGG CAA GGC AAA GAA AG-3`
<b>Mm_Myh7_reverse</b>	5`-TCA CCC CTG GAG ACT TTG TC-3`

Coll1a1 indicates collagen, type I, alpha 1; Col3a1, collagen, type III, alpha 1; Ctgf, connective tissue growth factor, Hprt, hypoxanthine-guanine phosphoribosyltransferase; Nppa, natriuretic peptide A; Nppb, B-type natriuretic factor; MuRF1, muscle RING-finger 1; Mapkapk, mitogen-activated protein kinase-activated protein kinase; Myh, myosin heavy chain.

**Table S2. GO-term analysis of upregulated proteins in DKO soleus muscle.**

<b>GO-term Biological process</b>	<b>Number of proteins</b>	<b>p-value</b>
Muscle organ development	5	2,26E-03
Muscle tissue development	3	6,88E-02
Myofibril assembly	2	5,84E-02
Actomyosin structure organization	2	7,62E-02
Proteolysis involved in cellular protein catabolic process	6	2,58E-02
Ubiquitin-dependent protein catabolic process	3	7,32E-02
Response to temperature stimulus	3	1,13E-02
Response to heat	3	4,56E-03

<b>GO-term Cellular component</b>	<b>Number of proteins</b>	<b>p-value</b>
Cytoskeleton	7	7,92E-02
Cullin-RING ubiquitin ligase complex	2	4,78E-02

<b>GO-term Molecular function</b>	<b>Number of proteins</b>	<b>p-value</b>
Ubiquitin protein ligase complex	2	4,13E-02
AMP binding	2	5,85E-02

**Table S3. GO-term analysis of downregulated proteins in DKO soleus muscle.**

<b>GO-term Biological process</b>	<b>Number of proteins</b>	<b>p-value</b>
Mitochondrion organization	3	5,49E-02
Mitochondrial transport	3	1,16E-02
Electron transport chain	7	4,59E-06
Cellular respiration	4	1,56E-03
Oxidation reduction	13	7,99E-06
Generation of precursor metabolites and energy	8	6,45E-05
Energy derivation by oxidation of organic compounds	4	6,56E-03
Fatty acid metabolic process	4	3,49E-03

<b>GO-term Cellular component</b>	<b>Number of proteins</b>	<b>p-value</b>
Mitochondrion	36	1,91E-17
Mitochondrial inner membrane	16	3,30E-11
Respiratory chain	5	3,99E-04
Mitochondrial lumen	6	1,78E-03
Mitochondrial matrix	6	1,78E-03

<b>GO-term Molecular function</b>	<b>Number of proteins</b>	<b>p-value</b>
Nucleoside binding	12	5,79E-02
Nucleotide binding	16	3,33E-02
Ribonucleotide binding	13	6,79E-02
Adenylnucleotide binding	12	5,30E-02
ATP binding	12	3,62E-02
Oxidoreductase activity, acting on heme group of donors	4	1,18E-04
Cytochrome-c oxidase activity	4	1,18E-04
Heme-copper terminal oxidase activity	4	1,18E-04
Methylcrotonyl-CoA carboxylase activity	2	8,41E-03
Electron carrier activity	4	5,33E-02
Hydrogen ion transmembrane transporter activity	4	4,96E-03
Inorganic cation transmembrane transporter activity	4	1,63E-02

## Supplementary Figures

### Fig. S1

**a** Immunoblotting of proteins from *gastrocnemius/plantaris* (GP) and *tibialis anterior* (TA) from control and DKO mice using anti-MuRF2 and anti-MuRF3 antibody, as indicated, confirmed absence of MuRF2 and/or MuRF3 proteins in the respective single and double knockout mice. Actin served as loading control. **b** Analysis of skeletal muscle mass of *gastrocnemius/plantaris* (GP) and *tibialis anterior* (TA) from control ( $n = 30$ ) and DKO ( $n = 26$ ) mice. Muscle weights were normalised to the tibia length. Data are shown as mean  $\pm$  SEM.

### Fig. S2

RT-PCR analysis of *MuRF1* (encoded by *Trim63*) gene expression in *soleus* (Sol), *extensor digitorum longus* (EDL), *gastrocnemius/plantaris* (GP) and *tibialis anterior* (TA) from control ( $n = 8-9$ ) and DKO ( $n = 4-6$ ) mice. *Hypoxanthine-guanine phosphoribosyltransferase* (*Hprt*) expression was used as reference. Data are represented as mean  $\pm$  SEM.

### Fig. S3

**a** Hematoxyline & eosin stain of cross-sections from *gastrocnemius/plantaris* (GP) and longitudinal sections from *tibialis anterior* (TA) from control and DKO mice. Subsarcolemmal accumulations of eosinophilic material occurred around a central core of myofibres in DKO muscles (arrow). Centrally localized nuclei are present in DKO but not control muscle (arrowhead). Scale bar, 50  $\mu$ m. **b** Gomori's Trichrome stain of cross-sections from *gastrocnemius/plantaris* (GP) and longitudinal sections from *tibialis anterior* (TA) from control and DKO mice. Protein aggregates (black and white arrows) are depicted.

### Fig. S4

Immunohistochemistry of cross-sections from *soleus* (Sol) and *extensor digitorum longus* (EDL) using anti-laminin (green) antibody. Filamentous actin was stained with phalloidin-labeled tetramethylrhodamine (TRITC, red) and nuclei were stained with 4',6-diamidino-2-phenylindole (DAPI; blue). Protein aggregations are indicated (arrow). Scale bar, 50  $\mu$ m.

### Fig. S5

Real-time RT-PCR analysis of *myosin heavy chain (Myh) -1, -2, -3, -4, and -7* expression in *gastrocnemius/plantaris (GP)* and *tibialis anterior (TA)* from control ( $n = 8$ ) and DKO ( $n = 4-6$ ) mice. *Hypoxanthine-guanine phosphoribosyltransferase (Hprt)* expression was used as reference. Data are represented as mean  $\pm$  SEM. \* $p < 0.05$ , \*\* $p < 0.01$ , \*\*\* $p < 0.001$ .

### Fig. S6

Maximal force development was measured in *soleus (Sol)* and *extensor digitorum longus (EDL)* of female control ( $n = 9$  each) and DKO (Sol,  $n = 12$ ; EDL,  $n = 11$ ) mice. Specific force [ $\text{mN}/\text{mm}^2$ ] per stimulation frequency [Hz] is shown. Data are depicted as mean  $\pm$  SEM. \* $p < 0.05$ , \*\* $p < 0.01$ , \*\*\* $p < 0.001$ .

### Fig. S7

**a** Real-time RT-PCR analysis of *MuRF1* (encoded by *Trim63*) gene expression in hearts of control ( $n = 8$ ) and DKO ( $n = 4$ ) mice. *Hprt* expression was used as reference. Data are represented as mean  $\pm$  SEM. **b** Real-time RT-PCR analysis of *connective tissue growth factor (Ctgf)* and *collagen, type I, alpha 1 (collagen 1; Coll1a1)*, and *collagen, type III, alpha 1 (collagen 3, Col3a1)* gene expression in hearts of control ( $n = 8$ ) and DKO ( $n = 4$ ) mice. *Hprt* expression was used as reference. Data are represented as mean  $\pm$  SEM.

### Fig. S8

Heterodimerization of MuRF-family members. **a** Rat cardiac myoblasts (H9c2-cells) were transfected with expression plasmids encoding pZsGreen-N1-MuRF1, pmCherry-N1-MuRF2, pZsGreen-N1-MuRF2, pmCherry-N1-MuRF3 alone or in combination as indicated. Filamentous actin was stained with tetramethylrhodamine-labeled phalloidin (TRITC, red) and nuclei were stained with 4',6-diamidino-2-phenylindole (DAPI, blue). MuRF1 and MuRF2 were predominantly cytoplasmatic, and MuRF3 resided at microtubuli. Scale bar, 10  $\mu\text{m}$ . **b** COS-7-cells were transfected with expression plasmids encoding FLAG- and/or Myc-tagged MuRF1, -2 and/or -3, as indicated. Input MuRF1, 2 and 3 proteins detected by immunoblot (IB) are shown. MuRF1, 2 and 3 proteins co-immunoprecipitated with their respective family members are shown in the bottom panel. **c** Mouse skeletal myoblasts (C2C12-cells) were transfected with expression plasmids encoding Myc-tagged MuRF1, -2 and/or -3 for 24, 48 or 72 h, as indicated.

**Fig. S9**

Heat-map of the Z-transformed p-values obtained by GO-analysis of proteins upregulated and downregulated in DKO muscle. The 30 % upregulated **a** and 30 % downregulated **b** proteins in DKO *soleus* were used for the Gene Ontology (GO) analysis with the DAVID online tool[3]. The obtained p-values of GO-terms cellular component  **$\alpha$**  and molecular function  **$\beta$**  that were significantly enriched ( $p < 0.05$ ) were log-transformed, Z-transformed, hierarchically clustered, and plotted as a heat map. *Color key* indicates p-values.

**Fig. 10**

KEGG pathway analysis of proteins involved in mitochondrial function downregulated in DKO muscle (oxidative phosphorylation). Proteins downregulated in DKO compared to control muscle are indicated (red asterisks).

**Fig. S11**

Peptide specific anti-MuRF2 and anti-MuRF3 antibody. Specificity of the anti-MuRF2 (top row) and anti-MuRF3 (bottom row) antibody from two immunizations (left and right panel each) was confirmed by western blot analyses using lysates from COS-7 cells transfected with expression plasmids encoding Myc-(His)<sub>6</sub>-tagged MuRF1, -2 or -3, as indicated.

**Fig. S12**

Immunoblotting of proteins from *gastrocnemius/plantaris* (GP), *tibialis anterior* (TA), *soleus* (Sol), *extensor digitorum longus* (EDL), *left ventricle* (LV), *right ventricle* (RV) (left panel) and various tissues (as indicated, right panel) from wild type mice using anti-MuRF2 or anti-MuRF3 antibody illustrate muscle specific expression pattern of MuRF proteins. Glyceraldehyde-3-phosphate dehydrogenase (GAPDH) served as control.

## References

1. Scharf M, Neef S, Freund R, Geers-Knorr C, Franz-Wachtel M, Brandis A, et al. Mitogen-activated protein kinase-activated protein kinases 2 and 3 regulate SERCA2a expression and fiber type composition to modulate skeletal muscle and cardiomyocyte function. *Mol Cell Biol.* 2013;33(13):2586-602.
2. Rappsilber J, Ishihama Y, Mann M. Stop and go extraction tips for matrix-assisted laser desorption/ionization, nanoelectrospray, and LC/MS sample pretreatment in proteomics. *Analytical chemistry.* 2003;75(3):663-70.
3. Huang da W, Sherman BT, Lempicki RA. Systematic and integrative analysis of large gene lists using DAVID bioinformatics resources. *Nat Protoc.* 2009;4(1):44-57.
4. Fielitz J, van Rooij E, Spencer JA, Shelton JM, Latif S, van der Nagel R, et al. Loss of muscle-specific RING-finger 3 predisposes the heart to cardiac rupture after myocardial infarction. *Proc Natl Acad Sci U S A.* 2007;104(11):4377-82.
5. Ronkina N, Kotlyarov A, Dittrich-Breiholz O, Kracht M, Hitti E, Milarski K, et al. The mitogen-activated protein kinase (MAPK)-activated protein kinases MK2 and MK3 cooperate in stimulation of tumor necrosis factor biosynthesis and stabilization of p38 MAPK. *Mol Cell Biol.* 2007;27(1):170-81.
6. Kim MS, Fielitz J, McAnally J, Shelton JM, Lemon DD, McKinsey TA, et al. Protein kinase D1 stimulates MEF2 activity in skeletal muscle and enhances muscle performance. *Mol Cell Biol.* 2008.
7. Fielitz J, Kim MS, Shelton JM, Latif S, Spencer JA, Glass DJ, et al. Myosin accumulation and striated muscle myopathy result from the loss of muscle RING finger 1 and 3. *J Clin Invest.* 2007;117(9):2486-95.
8. Bailey LE, Ong SD. Krebs-Henseleit solution as a physiological buffer in perfused and superfused preparations. *Journal of pharmacological methods.* 1978;1(2):171-5.
9. Brooks SV, Faulkner JA. Contractile properties of skeletal muscles from young, adult and aged mice. *J Physiol.* 1988;404:71-82.
10. Mutig N, Geers-Knoerr C, Piep B, Pahuja A, Vogt PM, Brenner B, et al. Lipoteichoic acid from *Staphylococcus aureus* directly affects cardiomyocyte contractility and calcium transients. *Mol Immunol.* 2013;56(4):720-8.
11. Grynkiewicz G, Poenie M, Tsien RY. A new generation of Ca<sup>2+</sup> indicators with greatly improved fluorescence properties. *J Biol Chem.* 1985;260(6):3440-50.
12. Primeaux SD, Tong M, Holmes GM. Effects of chronic spinal cord injury on body weight and body composition in rats fed a standard chow diet. *Am J Physiol Regul Integr Comp Physiol.* 2007;293(3):R1102-9.
13. Pankonien I, Alvarez JL, Doller A, Kohncke C, Rotte D, Regitz-Zagrosek V, et al. Ahnak1 is a tuneable modulator of cardiac Ca(v)1.2 calcium channel activity. *J Muscle Res Cell Motil.* 2011;32(4-5):281-90.